The Higgs boson decay into ZZ decaying to identical fermion pairs

T.V. Zagoskin[1,*] and A.Yu. Korchin[1,2,†]

[1] *NSC "Kharkov Institute of Physics and Technology", 61108 Kharkov, Ukraine*

[2] *V.N. Karazin Kharkov National University, 61022 Kharkov, Ukraine*

In order to investigate various decay channels of the Higgs boson h or the hypothetical dilaton, we consider a neutral particle X with zero spin and arbitrary CP parity. This particle can decay into two off-mass-shell Z bosons (Z_1^* and Z_2^*) decaying to identical fermion-antifermion pairs ($f\bar{f}$): $X \to Z_1^* Z_2^* \to f\bar{f}f\bar{f}$. We derive analytical formulas for the fully differential width of this decay and for the fully differential width of $h \to Z_1^* Z_2^* \to 4\ell$ (4ℓ stands for $4e$, 4μ, or $2e2\mu$). Integration of these formulas yields some Standard Model histogram distributions of the decay $h \to Z_1^* Z_2^* \to 4\ell$ which are compared with corresponding Monte Carlo simulated distributions obtained by ATLAS and with ATLAS experimental data.

arXiv:1701.06335v1 [hep-ph] 23 Jan 2017

I. INTRODUCTION

The boson h discovered [1] in 2012 by the CMS and ATLAS collaborations was reported to have a mass about 125 GeV and some decay modes predicted for the Standard Model (SM) Higgs boson. Since that time, the observed particle, called the Higgs boson, has been intensively studied (see, for example, papers [2]). A main goal of experiments on the Higgs boson physics has been to prove or disprove the hypothesis that h is the SM Higgs boson. Apart from the decay channels, the SM predicts that h has $J^{CP} = 0^{++}$. The followed thorough analysis has fine-tuned the mass of h, which is 125.09 ± 0.24 GeV according to Ref. [3], and has yielded some information on its spin and its CP parity.

In particular, the observation of the $h \to ZZ$ and $h \to W^-W^+$ modes (see, for example, Ref. [4]) means that the Higgs boson spin is 0, 1, or 2 while the fact that h decays [4] to $\gamma\gamma$ and the Landau-Yang theorem exclude the spin-one variant. Further, the analyses presented in [5, 6] rule out many spin-two hypotheses at a 99% confidence level (CL) or higher. Therefore, we conclude that the spin of the Higgs boson is 0 with a probability of about 99%.

To clarify the CP properties of h, in Ref. [7] we study the decay of a spin-zero particle X into two off-mass-shell Z bosons Z_1^* and Z_2^*. Since X is defined as an elementary neutral particle with zero spin, our study applies to the Higgs boson. Moreover, it can apply to the dilaton if this boson actually exists.

The amplitude of the decay $X \to Z_1^* Z_2^*$ depends (see Eq. (4) in [7]) on 3 complex-valued functions of the

*Electronic address: taras.zagoskin@gmail.com

†Electronic address: korchin@kipt.kharkov.ua

invariant masses of Z_1^* and Z_2^*. These functions determine the CP properties of the boson X and are called the XZZ couplings. Using the CMS and ATLAS experimental data on the decay $h \to Z_1^* Z_2^* \to 4\ell$ (where 4ℓ stands for $4e$, 4μ, or $2e2\mu$), these collaborations in Refs. [4–6] and we in Ref. [7] have obtained some constraints on the hZZ couplings. These constraints demonstrate that h is not a CP-odd state and it may be the SM Higgs boson, another CP-even state, or a boson with indefinite CP parity. Besides, as shown in [7], a non-zero imaginary part of the hZZ couplings is not excluded, which can be related to small loop corrections and possibly to a non-Hermiticity of the hZZ interaction.

Thus, the CP parity of the Higgs boson is not yet fully ascertained. Moreover, in some supersymmetric extensions of the SM there are [8–10] neutral bosons with negative or indefinite CP parity. That is why it is now important to establish the CP properties of the Higgs boson.

Aiming at that, we consider the decay of the particle X into Z_1^* and Z_2^* which then decay to fermion-antifermion pairs $f_1\bar{f}_1$ and $f_2\bar{f}_2$ respectively. While in Ref. [7] we study in detail the decays with the non-identical fermions, $f_1 \neq f_2$, in the present paper the case $f_1 = f_2$ is under investigation. The masses of the fermions f_1 and f_2 is neglected in both papers.

We are motivated to consider the decay into identical fermions by the following. In Refs. [5, 6] the CMS and ATLAS collaborations analyze 95 decays $h \to Z_1^* Z_2^* \to 4\ell$. 53 of them are the decays to identical leptons, namely to $4e$ or 4μ. In spite of the fact that the decays to the identical leptons make up about 55% of the measured decays $h \to Z_1^* Z_2^* \to 4\ell$, the distributions of the former decays have not been properly analytically studied. The SM total widths of the decays into identical fermions are studied in Refs. [11, 12] and are calculated in [13]. Some distributions of the decay $X \to Z_1^* Z_2^* \to 4\ell$ are plotted in [5, 6] for the SM Higgs boson and some spin-zero states beyond the SM . In the present paper we perform a more general study and consider the decay $X \to Z_1^* Z_2^* \to f\bar{f}f\bar{f}$ with allowance for all the possible CP properties of the particle X.

In Sec. II we derive an analytical formula for the fully differential width of the decay to identical fermions. Section III shows a comparison of some distributions of the decay to identical leptons with those for the decay into non-identical ones. For this comparison we obtain an exact analytical formula for a certain differential width of the decay to non-identical fermions (see Appendix B). We analyze the usefulness of all the compared distributions for obtaining constraints on the hZZ couplings. In Sec. IV we derive some SM histogram distributions of the decay $h \to Z_1^* Z_2^* \to 4\ell$ by Monte Carlo (MC) integration and compare them with the corresponding simulations presented in Ref. [5] and with the experimental distributions from [5].

II. THE FULLY DIFFERENTIAL WIDTH

We consider a neutral particle X with zero spin and arbitrary CP parity. It can decay into two fermion-antifermion pairs, $f_1\bar{f}_1$ and $f_2\bar{f}_2$, through the two off-mass-shell Z bosons (Z_1^* and Z_2^*):

$$X \to Z_1^* Z_2^* \to f_1\bar{f}_1 f_2\bar{f}_2. \tag{1}$$

If $m_X \in (4m_b, 2m_t]$ (m_X is the mass of the particle X, m_b is the mass of the b quark, m_t is the mass of the t quark), which holds for $X = h$, then $f_j = e^-, \mu^-, \tau^-, \nu_e, \nu_\mu, \nu_\tau, u, c, d, s, b$. If $m_X > 4m_t$, which is possible [14] if X is the dilaton, then f_j can be the top quark as well.

In Ref. [7] we considered decays

$$X \to Z_1^* Z_2^* \to f_1\bar{f}_1 f_2\bar{f}_2, \qquad f_1 \neq f_2 \tag{2}$$

at the tree level.

The present paper shows our analysis of decay (1) in the case of the identical fermions, $f_1 = f_2 \equiv f$:

$$X \to Z_1^* Z_2^* \to f\bar{f}f\bar{f}. \tag{3}$$

The matrix element of decay (3) is

$$M_{iden} = M - \tilde{M}, \tag{4}$$

where the matrix elements M and $\tilde{M}$ correspond to the diagrams (a) and (b) in Fig. 1 respectively. Namely,

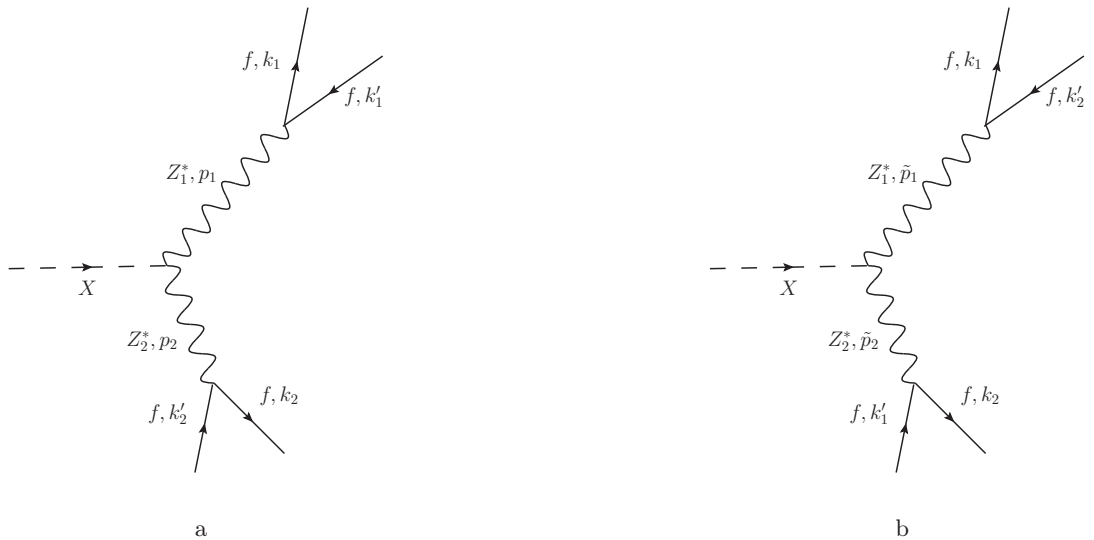

Figure 1: The Feynman diagrams contributing to the matrix element of decay (3).

$$M = \frac{i}{(a_1 - m_Z^2 + im_Z\Gamma_Z)(a_2 - m_Z^2 + im_Z\Gamma_Z)} \times$$
$$\times \sum_{\lambda_1,\lambda_2=-1,0,1} A_{X\to Z_1^* Z_2^*}(p_1, p_2, \lambda_1, \lambda_2) A_{Z\to f\bar{f}}(k_1, k_1', \lambda_{f_1}, \lambda_{\bar{f}_1}, \lambda_1) A_{Z\to f\bar{f}}(k_2, k_2', \lambda_{f_2}, \lambda_{\bar{f}_2}, \lambda_2),$$
$$\tilde{M} = \frac{i}{(\tilde{a}_1 - m_Z^2 + im_Z\Gamma_Z)(\tilde{a}_2 - m_Z^2 + im_Z\Gamma_Z)} \times$$
$$\times \sum_{\lambda_1,\lambda_2=-1,0,1} A_{X\to Z_1^* Z_2^*}(\tilde{p}_1, \tilde{p}_2, \lambda_1, \lambda_2) A_{Z\to f\bar{f}}(k_1, k_2', \lambda_{f_1}, \lambda_{\bar{f}_2}, \lambda_1) A_{Z\to f\bar{f}}(k_2, k_1', \lambda_{f_2}, \lambda_{\bar{f}_1}, \lambda_2), \quad (5)$$

where

- k_1 and k_1' (k_2 and k_2') are the 4-momenta of the particles f_1 and $\bar{f}_1$ (f_2 and $\bar{f}_2$) in the rest frame of X;
- $p_1 \equiv k_1 + k_1'$ and $p_2 \equiv k_2 + k_2'$ are the 4-momenta of Z_1^* and Z_2^* respectively in the rest frame of X in diagram Fig. 1 (a);
- $a_j \equiv p_j^2$;
- m_Z and Γ_Z are respectively the pole mass and the total width of the Z boson;
- $A_{X\to Z_1^* Z_2^*}(p_1, p_2, \lambda_1, \lambda_2)$ is the amplitude of the decay $X \to Z_1^* Z_2^*$ where p_j and λ_j are respectively the momentum and the helicity of the boson Z_j^* in the rest frame of X;
- $A_{Z\to f\bar{f}}(k, k', \lambda_f, \lambda_{\bar{f}}, \lambda)$ is the amplitude of the decay $Z \to f\bar{f}$ where k and λ_f (k' and $\lambda_{\bar{f}}$) are respectively the momentum and the polarization of f ($\bar{f}$) in the rest frame of Z, λ is the helicity of decaying Z;
- $\tilde{p}_1 \equiv k_1 + k_2'$ and $\tilde{p}_2 \equiv k_2 + k_1'$ are the 4-momenta of Z_1^* and Z_2^* respectively in the rest frame of X in diagram Fig. 1 (b);
- $\tilde{a}_j \equiv \tilde{p}_j^2$.

From the conservation of the energy-momentum 4-vectors we find all the possible values of a_1 and a_2:

$$4m_{f_1}^2 < a_1 < (m_X - 2m_{f_2})^2, \qquad 4m_{f_2}^2 < a_2 < (m_X - \sqrt{a_1})^2, \quad (6)$$

where m_{f_j} is the mass of the fermion f_j.

The amplitude $A_{X\to Z_1^* Z_2^*}(p_1, p_2, \lambda_1, \lambda_2)$ is [7]

$$A_{X\to Z_1^* Z_2^*}(p_1, p_2, \lambda_1, \lambda_2) = g_Z \Bigg(a_Z(a_1, a_2)(e_1^* \cdot e_2^*) + \frac{b_Z(a_1, a_2)}{m_X^2}(e_1^* \cdot p_X)(e_2^* \cdot p_X)$$
$$+ i\frac{c_Z(a_1, a_2)}{m_X^2}\varepsilon_{\mu\nu\rho\sigma} p_X^\mu (p_1^\nu - p_2^\nu)(e_1^\rho)^*(e_2^\sigma)^* \Bigg), \quad (7)$$

where $g_Z \equiv 2\sqrt{\sqrt{2}G_F}m_Z^2$, G_F is the Fermi constant, $a_Z(a_1, a_2)$, $b_Z(a_1, a_2)$, and $c_Z(a_1, a_2)$ are some complex-valued dimensionless functions of a_1 and a_2, $e_j \equiv e(p_j, \lambda_j)$, $e(p, \lambda)$ is the polarization 4-vector of the Z boson with

a momentum p and a helicity λ, $p_X \equiv p_1 + p_2 = \tilde{p}_1 + \tilde{p}_2 = (m_X, \vec{0})$ is the 4-momentum of the boson X in its own rest frame, $\varepsilon_{\mu\nu\rho\sigma}$ is the Levi-Civita symbol ($\varepsilon_{0123} = 1$).

The values of the couplings a_Z, b_Z, and c_Z reflect the CP properties of the particle X. Specifically, at the tree level the correspondence shown in Table I takes place.

Table I: The CP parity of the particle X for various values of a_Z, b_Z, and c_Z.

CP_X	a_Z	b_Z	c_Z
1	any	any	0
-1	0	0	$\neq 0$
indefinite	$\neq 0$	any	$\neq 0$
	any	$\neq 0$	$\neq 0$

For the SM Higgs boson the loop corrections change slightly the tree-level values $a_Z = 1$, $b_Z = 0$, $c_Z = 0$ (see, for example, Refs. [6, 15–17]). In particular, the SM electroweak radiative diagrams tune the value of the coupling b_Z, beginning from the next-to-leading order, while a contribution to c_Z appears at the three-loop level. Physics beyond the SM is the additional source of a possible deviation from the values $a_Z = 1$, $b_Z = 0$, $c_Z = 0$.

Calculating Lorentz-invariant amplitude (7) in the rest frame of X, we derive that

$$
\begin{aligned}
&A_{X\to Z_1^* Z_2^*}(p_1, p_2, \pm 1, \pm 1) = g_Z \left(a_Z(a_1, a_2) \pm c_Z(a_1, a_2) \frac{k}{m_X^2} \right), \\
&A_{X\to Z_1^* Z_2^*}(p_1, p_2, 0, 0) = -g_Z \left(a_Z(a_1, a_2) \frac{m_X^2 - a_1 - a_2}{2\sqrt{a_1 a_2}} + b_Z(a_1, a_2) \frac{k^2}{4 m_X^2 \sqrt{a_1 a_2}} \right), \\
&A_{X\to Z_1^* Z_2^*}(p_1, p_2, \lambda_1, \lambda_2) = 0, \qquad \lambda_1 \neq \lambda_2,
\end{aligned}
\tag{8}
$$

where $k(a_1, a_2) \equiv \lambda^{1/2}(m_X^2, a_1, a_2)$, $\lambda(x, y, z) \equiv x^2 + y^2 + z^2 - 2xy - 2xz - 2yz$.

We take the amplitude $A_{Z\to f\bar{f}}(k, k', \lambda_f, \lambda_{\bar{f}}, \lambda)$ from the SM (see, for example, Ref. [18]).

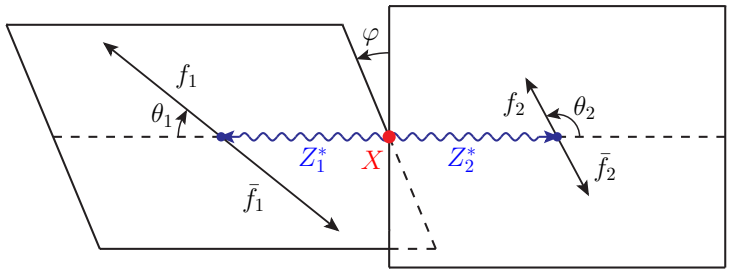

Figure 2: The kinematics of decay (1). We show the momenta of Z_1^* and Z_2^* in the rest frame of X while the momenta of f_1 and $\bar{f}_1$ (f_2 and $\bar{f}_2$) are shown in the rest frame of Z_1^* (Z_2^*).

Further, to describe decay (1), let us introduce the following angles (see Fig. 2): θ_1 (θ_2) is the angle between

the momentum of Z_1^* (Z_2^*) in the rest frame of X and the momentum of f_1 (f_2) in the rest frame of Z_1^* (Z_2^*) (in other words, θ_1 (θ_2) is the polar angle of the fermion f_1 (f_2)) and φ is the azimuthal angle between the planes of the decays $Z_1^* \to f_1\bar{f}_1$ and $Z_2^* \to f_2\bar{f}_2$. For decay (3), we can arbitrarily choose the Z boson which we will call Z_1^*, and then we will refer to the other Z boson as Z_2^*.

As for $\tilde{a}_1$ and $\tilde{a}_2$, an explicit calculation yields

$$\begin{aligned}\tilde{a}_1 &= \frac{m_X^2 - a_1 - a_2}{4}(1 - \cos\theta_1\cos\theta_2) + \frac{\sqrt{a_1 a_2}}{2}\sin\theta_1\sin\theta_2\cos\phi + \frac{k}{4}(\cos\theta_1 - \cos\theta_2),\\ \tilde{a}_2 &= \frac{m_X^2 - a_1 - a_2}{4}(1 - \cos\theta_1\cos\theta_2) + \frac{\sqrt{a_1 a_2}}{2}\sin\theta_1\sin\theta_2\cos\phi + \frac{k}{4}(\cos\theta_2 - \cos\theta_1).\end{aligned} \tag{9}$$

The expression for the amplitude $A_{X\to Z_1^* Z_2^*}(\tilde{p}_1, \tilde{p}_2, \lambda_1, \lambda_2)$ is analogous to Eq. (7):

$$\begin{aligned}A_{X\to Z_1^* Z_2^*}(\tilde{p}_1, \tilde{p}_2, \lambda_1, \lambda_2) =& g_Z\Bigg(a_Z(\tilde{a}_1, \tilde{a}_2)(E_1^* \cdot E_2^*) + \frac{b_Z(\tilde{a}_1, \tilde{a}_2)}{m_X^2}(E_1^* \cdot p_X)(E_2^* \cdot p_X)\\ &+ i\frac{c_Z(\tilde{a}_1, \tilde{a}_2)}{m_X^2}\varepsilon_{\mu\nu\rho\sigma}p_X^\mu(\tilde{p}_1^\nu - \tilde{p}_2^\nu)(E_1^\rho)^*(E_2^\sigma)^*\Bigg),\end{aligned} \tag{10}$$

where $\tilde{e}_j = e(\tilde{p}_j, \lambda_j)$. Calculating $A_{X\to Z_1^* Z_2^*}(\tilde{p}_1, \tilde{p}_2, \lambda_1, \lambda_2)$ in the rest frame of X, we get

$$\begin{aligned}&A_{X\to Z_1^* Z_2^*}(\tilde{p}_1, \tilde{p}_2, \pm 1, \pm 1) = g_Z\left(a_Z(\tilde{a}_1, \tilde{a}_2) \pm c_Z(\tilde{a}_1, \tilde{a}_2)\frac{2}{m_X}|\mathbf{k}_1 + \mathbf{k}_2'|\right),\\ &A_{X\to Z_1^* Z_2^*}(\tilde{p}_1, \tilde{p}_2, 0, 0) = -\frac{g_Z}{4\sqrt{\tilde{a}_1\tilde{a}_2}}\Bigg(a_Z(\tilde{a}_1, \tilde{a}_2)\Big(m_X^2 + a_1 + a_2 + (m_X^2 - a_1 - a_2)\cos\theta_1\cos\theta_2\\ &- 2\sqrt{a_1 a_2}\sin\theta_1\sin\theta_2\cos\phi\Big) + b_Z(\tilde{a}_1, \tilde{a}_2)\cdot 4|\mathbf{k}_1 + \mathbf{k}_2'|^2\Bigg),\\ &A_{X\to Z_1^* Z_2^*}(\tilde{p}_1, \tilde{p}_2, \lambda_1, \lambda_2) = 0, \qquad \lambda_1 \neq \lambda_2,\end{aligned} \tag{11}$$

where

$$|\mathbf{k}_1 + \mathbf{k}_2'|^2 = \frac{a_1 + a_2}{4} - \frac{\sqrt{a_1 a_2}}{2}\sin\theta_1\sin\theta_2\cos\phi + \frac{k^2}{16m_X^2}(\cos^2\theta_1 + \cos^2\theta_2) + \frac{\cos\theta_1\cos\theta_2}{8m_X^2}(m_X^4 - (a_1 - a_2)^2). \tag{12}$$

Using Eqs. (4), (5), (8), (9), and (11), we derive Eq. (A1) (see Appendix A).

III. INVARIANT MASS AND ANGULAR DISTRIBUTIONS

Integrating Eq. (A1) numerically, we can obtain some distributions of decay (3). Moreover, numerical integration of Eq. (5) in Ref. [7] yields distributions for decay (2). In Figs. 3 and 4 we compare certain distributions of (3) with those of (2). We define the weak mixing angle as $\theta_W \equiv \arcsin\sqrt{1 - m_W^2/m_Z^2}$, where m_W is the mass of the W boson, and use the values of the constants in Table II neglecting their experimental uncertainties.

First, we show the SM distribution $\frac{1}{\Gamma}\frac{d^2\Gamma}{da_1 da_2}$ for any decay $h \to Z_1^* Z_2^* \to f_1\bar{f}_1 f_2\bar{f}_2$ with f_1 different from f_2 (see Fig. 3a) and that for any decay $h \to Z_1^* Z_2^* \to 4l$ where l stands for e, μ, or τ (see Fig. 3b). We see peaks at $\sqrt{a_1} = m_Z$ or $\sqrt{a_2} = m_Z$ and a flat surface outside the peaks for either dependence. For the decay into

Table II: The values of the Fermi constant, of the masses of h, Z, W, and of the total width of Z from Ref. [19].

$G_F = 1.1663787(6) \times 10^{-5}$ GeV^{-2}
$m_h = 125.7(4)$ GeV
$m_Z = 91.1876(21)$ GeV
$m_W = 80.385(15)$ GeV
$\Gamma_Z = 2.4952(23)$ GeV

non-identical fermions the SM values of $\frac{1}{\Gamma}\frac{d^2\Gamma}{da_1 da_2}$ on the peaks are about 120 times greater than the values on the "plateau" (the square $\sqrt{a_1}, \sqrt{a_2} \lesssim 50$ GeV). However, for the decay into identical leptons this ratio varies from 3 to 55 if we take $\sqrt{a_1} = m_Z$, $\sqrt{a_2} = \frac{1}{2}(m_h - m_Z)$ as the indicative point on the peak and on the plateau we consider the points on the line $\sqrt{a_1} = \sqrt{a_2}$ from $\sqrt{a_1} = 1$ GeV to $\sqrt{a_1} = 59$ GeV. Moreover, the SM probability that in a decay $h \to Z_1^* Z_2^* \to f_1\bar{f}_1 f_2 \bar{f}_2$ either Z boson has an invariant mass less than 50 GeV is

$$\frac{1}{\Gamma_{f_1 \neq f_2}|_{SM}} \int\limits_0^{(50\ \mathrm{GeV})^2} da_1 \int\limits_0^{(50\ \mathrm{GeV})^2} da_2 \left.\frac{d^2\Gamma_{f_1 \neq f_2}}{da_1 da_2}\right|_{SM} \approx 2.4\% \tag{13}$$

while the corresponding probability for the decay $h \to Z_1^* Z_2^* \to 4l$ is much higher, of about 21%.

Figure 4 shows the distributions $\frac{1}{\Gamma}\frac{d\Gamma}{da}$, $\frac{1}{\sin\theta}\frac{1}{\Gamma}\frac{d\Gamma}{d\theta}$, and $\frac{1}{\Gamma}\frac{d\Gamma}{d\phi}$ for the decay to non-identical leptons and the decay to identical ones. The definitions and explicit formulas for the differential widths $\frac{d\Gamma}{da}$ and $\frac{d\Gamma}{d\theta}$ are given in Appendix C (see Eqs. (C1), (C9), (C10), and (C15)).

The distributions in Fig. 4 are presented at the following four sets of values of the couplings a_Z, b_Z, and c_Z:

$$\begin{aligned}
&|a_Z| = 1,\ b_Z = 0,\ c_Z = 0,\\
&a_Z = 1,\ b_Z = 0,\ c_Z = 0.5,\\
&a_Z = 1,\ b_Z = 0,\ c_Z = 0.5\,i,\\
&a_Z = 1,\ b_Z = -0.5,\ c_Z = 0.
\end{aligned} \tag{14}$$

In Ref. [7] sets (14) are shown to be consistent with the available LHC data and are chosen for an analysis of some observables sensitive to the hZZ couplings.

The dependences in the upper plot of Fig. 4a are calculated using Eq. (A2) from Ref. [7] and Eq. (B2) from this paper. The dots in the two other plots of Fig. 4a present the results of MC integrations of Eq. (A2). The lines shown in these plots fit the corresponding dots according to the method of least squares.

The dots in Fig. 4b are obtained by means of MC integration of Eq. (A1). The lines in the upper plot of Fig. 4b consist of cubic parabolas joining the neighboring dots, since we have not been able to properly fit the dots of this plot with the method of least squares. The lines in the two other plots of Fig. 4b are least-squares fits to the corresponding dots.

The dependences plotted in Fig. 4 almost coincide at all four sets (14). For this reason, we can get significant

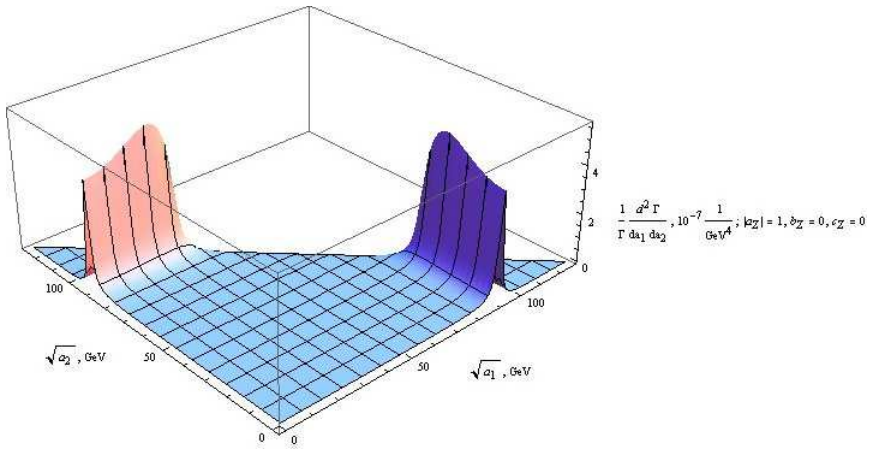

a

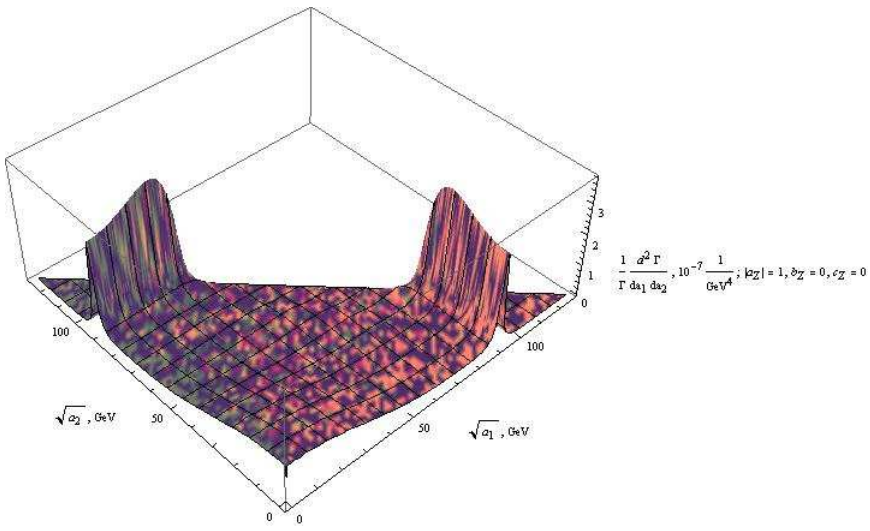

b

Figure 3: The distribution $\frac{1}{\Gamma}\frac{d^2\Gamma}{da_1 da_2}$ in the SM for the decays $h \to Z_1^* Z_2^* \to f_1\bar{f}_1 f_2\bar{f}_2$ with $f_1 \neq f_2$ (a) and for the decays $h \to Z_1^* Z_2^* \to 4l$ with $l = e, \mu, \tau$ (b).

constraints on a_Z, b_Z, and c_Z via measurement of the distributions $\frac{1}{\Gamma}\frac{d\Gamma}{da}$, $\frac{1}{\sin\theta}\frac{1}{\Gamma}\frac{d\Gamma}{d\theta}$, and $\frac{1}{\Gamma}\frac{d\Gamma}{d\phi}$ only if these distributions are measured at very high precision. That is why in order to constrain the hZZ couplings, we should try to define observables sensitive to these couplings, like it is done in [7] for decay (2).

The distinctions between the distributions $\frac{1}{\Gamma}\frac{d\Gamma}{da}$ for the decay into non-identical leptons (Fig. 4a) and those for identical leptons (Fig. 4b) are due to greater values of the SM distribution $\frac{1}{\Gamma}\frac{d^2\Gamma}{da_1 da_2}$ on the plateau for the decay $h \to Z_1^* Z_2^* \to 4l$ and smaller values of this distribution at the peaks $\sqrt{a_1} = m_Z$ and $\sqrt{a_2} = m_Z$ (see Fig. 3). However, these distinctions are insubstantial.

The dissimilarity between the functions $\frac{1}{\sin\theta}\frac{1}{\Gamma}\frac{d\Gamma}{d\theta}$ and $\frac{1}{\Gamma}\frac{d\Gamma}{d\phi}$ in Figs. 4a and 4b is much more appreciable. The global maximum of $\frac{1}{\sin\theta}\frac{1}{\Gamma}\frac{d\Gamma}{d\theta}$ at $\theta = \pi/2$ in Fig. 4a becomes a local minimum in Fig. 4b, and the values near the points $\theta = 0$ and $\theta = \pi$ increase. Analogous distinctions take place between the dependences of $\frac{1}{\Gamma}\frac{d\Gamma}{d\phi}$ in Figs. 4a and 4b.

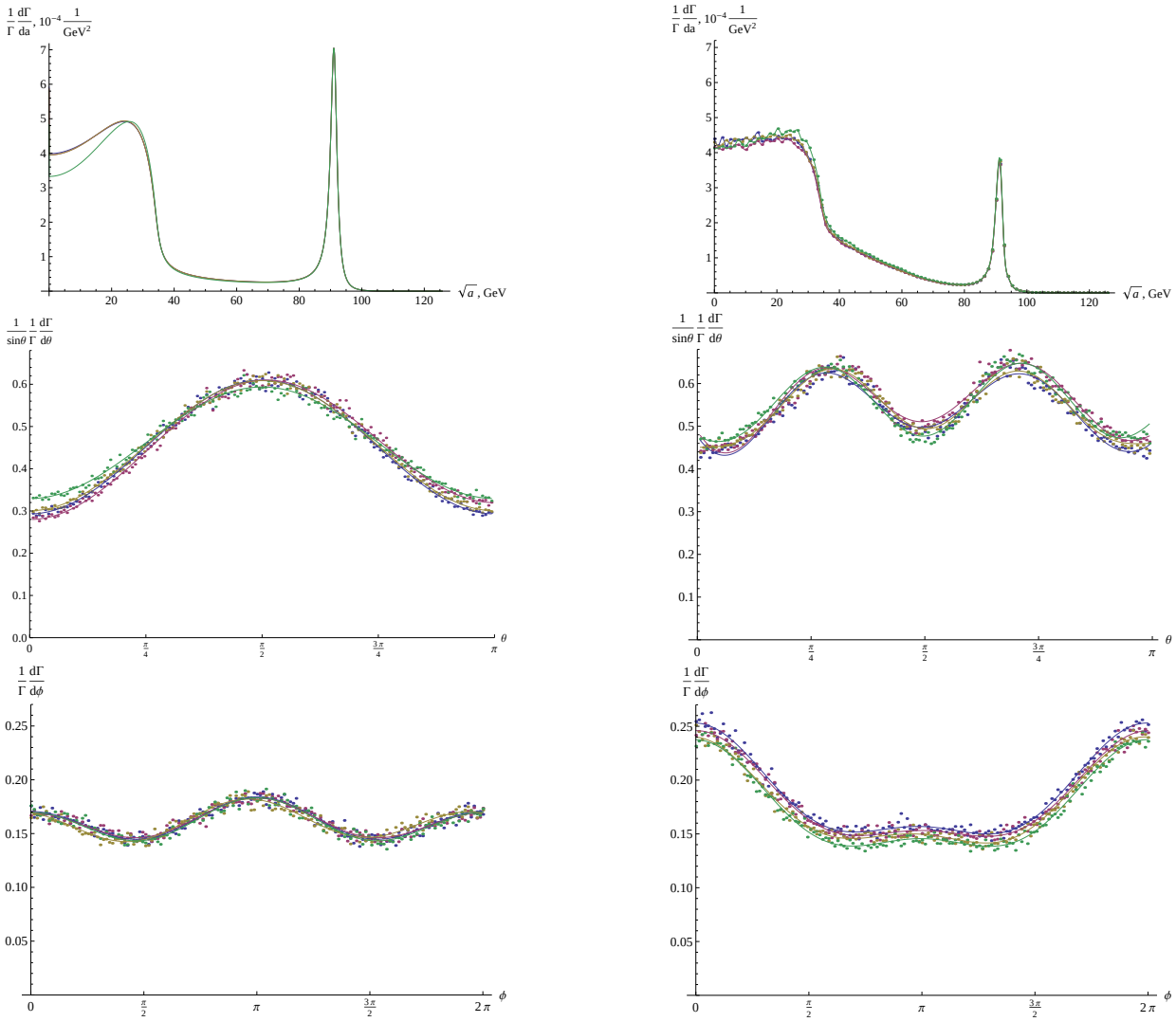

a b

Figure 4: The distributions $\frac{1}{\Gamma}\frac{d\Gamma}{da}$, $\frac{1}{\sin\theta}\frac{1}{\Gamma}\frac{d\Gamma}{d\theta}$, and $\frac{1}{\Gamma}\frac{d\Gamma}{d\phi}$ for the decays $h \to Z_1^* Z_2^* \to l_1^- l_1^+ l_2^- l_2^+$; $l_j = e, \mu, \tau$ in the cases $l_1 \neq l_2$ (a) and $l_1 = l_2$ (b). The blue, purple, yellow, and green lines and dots correspond to sets (14) respectively.

IV. COMPARISON WITH EXPERIMENTAL DATA

A. ATLAS and CMS results

In Ref. [5] the ATLAS collaboration presents experimental distributions of the decay $h \to Z_1^* Z_2^* \to 4\ell$ and corresponding distributions derived with MC simulations in the SM. We take the same kinematic limitations and the bin widths as ATLAS and use Eqs. (A1) and (A2) to derive the SM histogram distributions of the decay $h \to Z_1^* Z_2^* \to 4\ell$ which appear in [5]. Comparison of our distributions with the ATLAS experimental and theoretical ones will determine the usefulness of Eq. (A1).

CMS has shown experimental distributions for the decay $h \to VV \to 4\ell$ ($VV = ZZ$, $Z\gamma$, $\gamma\gamma$) and corresponding MC simulations in the SM in Ref. [6]. Taking the same kinematic limitations and the same bin widths as CMS, we integrate Eqs. (A1) and (A2) in the SM to obtain distributions for the decay $h \to Z_1^* Z_2^* \to 4\ell$.

We introduce the four following variables: m_{12} (m_{34}) is the invariant mass of the Z boson which is produced in

a decay $h \to Z_1^* Z_2^* \to 4\ell$ and whose mass is closest to (most distant from) m_Z, θ_1' (θ_2') is the polar angle of the fermion whose parent Z boson has the invariant mass closest to (most distant from) m_Z. From the definitions of m_{12} and m_{34} it follows that

$$|m_{12} - m_Z| < |m_{34} - m_Z|. \tag{15}$$

However, since $m_h < 2\, m_Z$, the quantity m_{12} (m_{34}) can be equivalently defined as the invariant mass of the heaviest (lightest) Z boson produced in a decay $h \to Z_1^* Z_2^* \to 4\ell$ ($m_{12} > m_{34}$).

In Ref. [5] ATLAS shows distributions of m_{12}, m_{34}, $\cos\theta_1'$, and ϕ (a distribution of $\cos\theta_2'$ is not presented). ATLAS selects decays $h \to Z_1^* Z_2^* \to 4\ell$ wherein

$$m_{12} \in (50\ \text{GeV}, 106\ \text{GeV}), \qquad m_{34} \in (12\ \text{GeV}, 115\ \text{GeV}), \qquad \eta_e \in (-2.47, 2.47), \qquad \eta_\mu \in (-2.7, 2.7). \tag{16}$$

Here η_e (η_μ) is the pseudorapidity of the electron (muon):

$$\eta_i(\theta_i) \equiv -\ln\tan\frac{\theta_i}{2}, \qquad i = e, \mu, \tag{17}$$

where θ_e (θ_μ) is the polar angle of the electron (muon).

CMS paper [6] presents distributions of m_{12}, m_{34}, $\cos\theta_1'$, $\cos\theta_2'$, and ϕ for the decay $h \to VV \to 4\ell$ with

$$m_{12} \in (40\ \text{GeV}, 120\ \text{GeV}), \qquad m_{34} \in (12\ \text{GeV}, 120\ \text{GeV}), \qquad \eta_e \in (-2.5, 2.5), \qquad \eta_\mu \in (-2.4, 2.4). \tag{18}$$

Constraints (16) and (18) determine the fractions of decays selected by ATLAS or CMS in the corresponding decay modes. These fractions are given by the left-hand sides of Eqs. (D1) and (D9). We have calculated the corresponding percentages in the SM (see Table III).

Table III: The SM percentages P_{SM} of decays selected by the CMS and ATLAS collaborations, for various decay modes.

Decay mode	P_{SM}	
	CMS	ATLAS
$h \to Z_1^* Z_2^* \to 4e$	84.6 %	75.6 %
$h \to Z_1^* Z_2^* \to 4\mu$	84.1 %	76.4 %
$h \to Z_1^* Z_2^* \to 2e2\mu$	86.5 %	85.1 %
$h \to Z_1^* Z_2^* \to 4\ell$	85.5 %	81.1 %

B. A discussion of plots

Integrating Eq. (D10) with a MC method, we derive some SM histogram distributions of the decay $h \to Z_1^* Z_2^* \to 4\ell$ (see the blue lines in Figs. 5 and 6). The bin widths in Fig. 5 are taken from Ref. [5] while those in Fig. 6 are taken from [6].

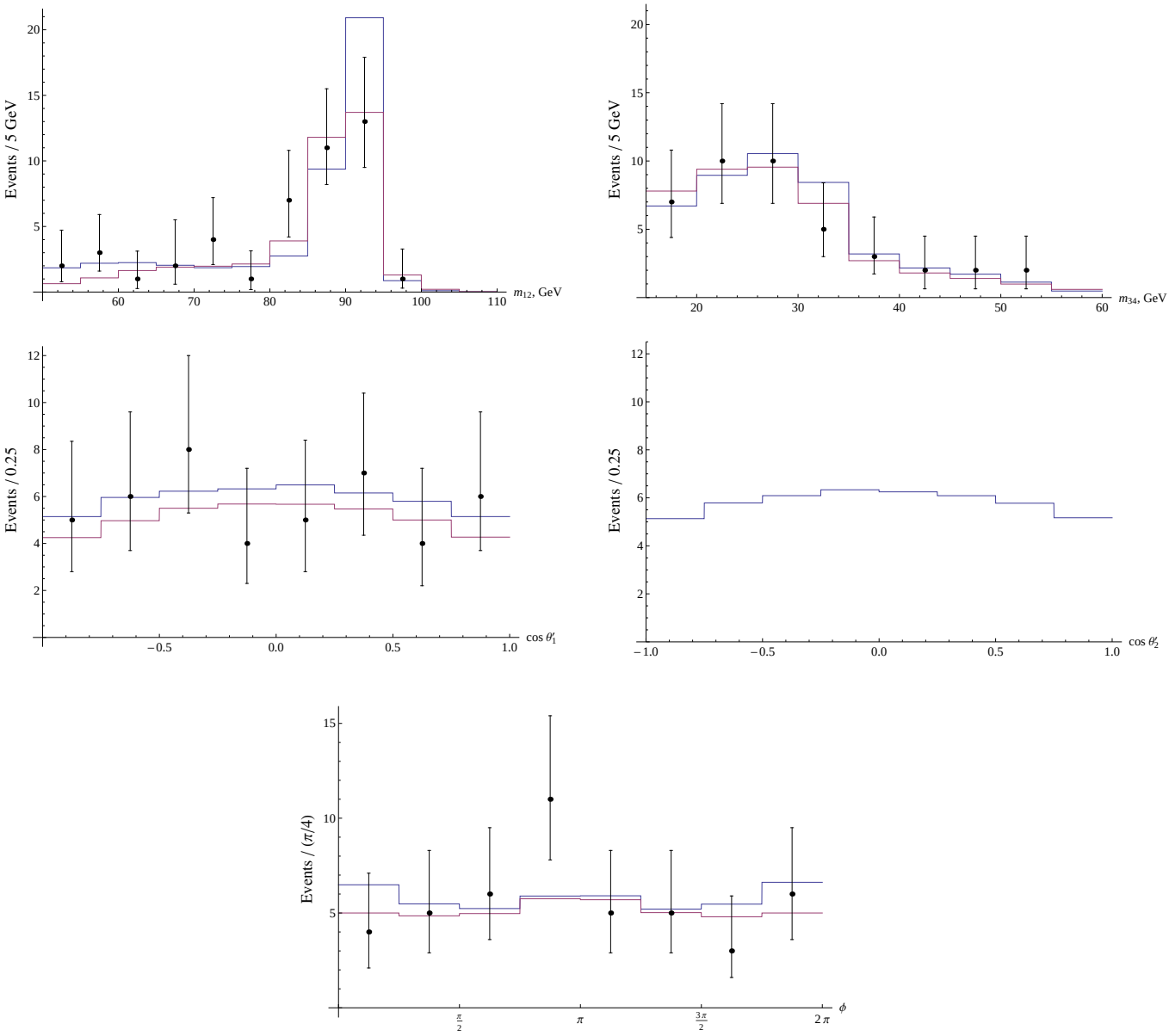

Figure 5: The numbers of decays $h \to Z_1^* Z_2^* \to 4\ell$ in bins of m_{12}, m_{34}, $\cos\theta_1'$, $\cos\theta_2'$, and ϕ according to our calculations in the SM (blue lines), the ATLAS (Ref. [5]) MC simulations in the SM (purple lines), and the ATLAS experimental data in [5] (points with error bars). In our computations the total number of decays $h \to Z_1^* Z_2^* \to 4\ell$ is chosen to be 45. Both our calculations and the ATLAS MC simulations are carried out for ATLAS limitations (16).

ATLAS reports about 45 decays $h \to Z_1^* Z_2^* \to 4\ell$ with $m_{4\ell} \in (115\,\text{GeV}, 130\,\text{GeV})$ ($m_{4\ell}$ is the invariant mass of the 4 final leptons) in Ref. [5] (see Table 3 there). For this reason, we have calculated our distributions shown in Fig. 5, setting $N_{4\ell}^{\text{ATLAS}} = 45$ in Eq. (D10).

It is of interest to sum up the numbers of decays over all the bins for each plot in Fig. 5 (see Table IV).

The total number of the decays in the ATLAS experimental distribution of m_{34} is 41. That is why 4 decays measured by ATLAS are not presented in this distribution. Therefore, in these decays $m_{34} \in (12\,\text{GeV}, 15\,\text{GeV})$ (see ATLAS limitations (16) and Fig. 5). The bin sum 41.14 for the ATLAS simulated distribution of m_{34} is notably closer to 41 than the bin sum 43.31 for our distribution of m_{34}.

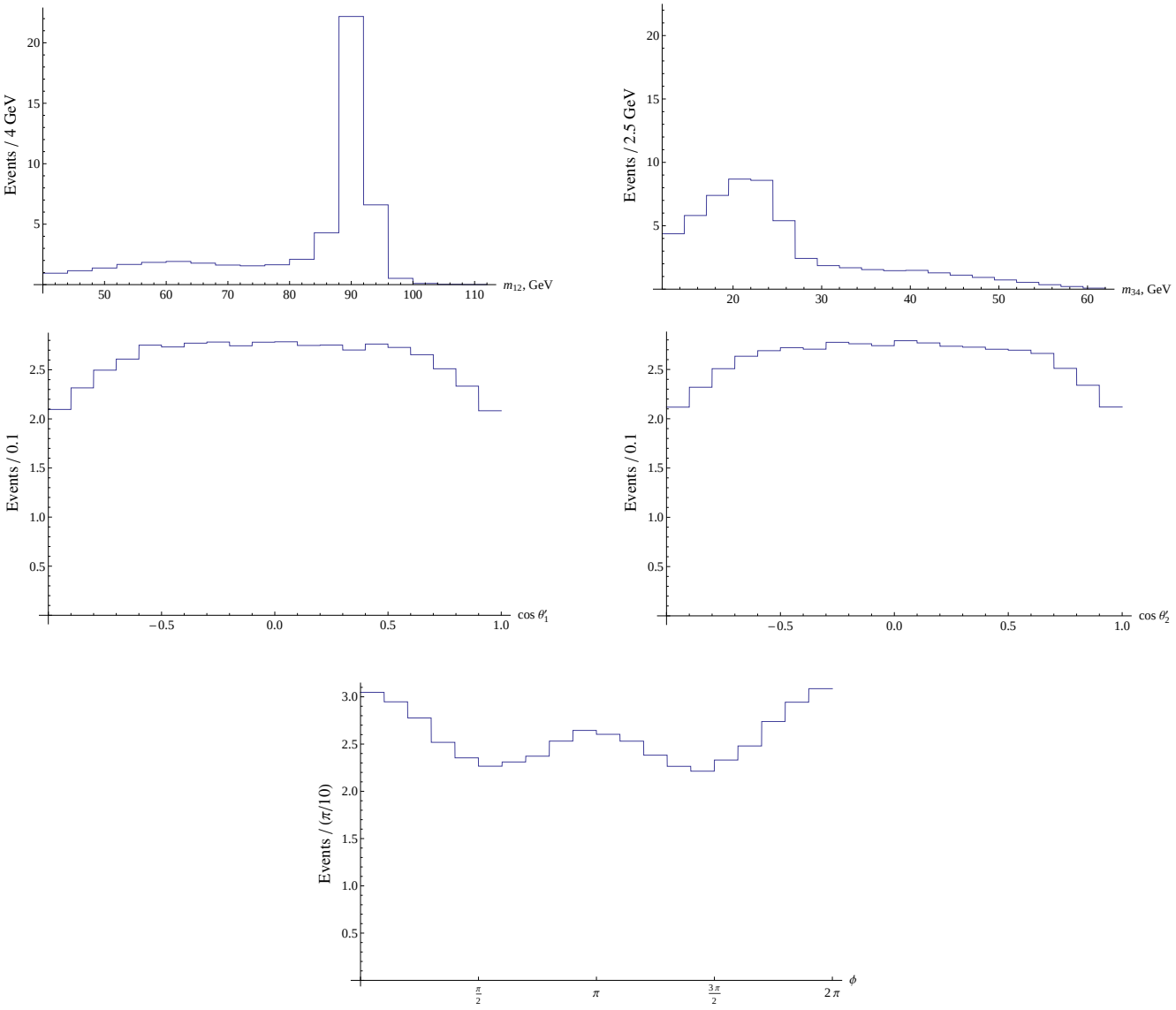

Figure 6: The numbers of decays $h \to Z_1^* Z_2^* \to 4\ell$ in bins of m_{12}, m_{34}, $\cos\theta_1'$, $\cos\theta_2'$, and ϕ according to our calculations in the SM. The total number of decays $h \to Z_1^* Z_2^* \to 4\ell$ is chosen to be 50. Our computations are performed for CMS limitations (18).

For the ATLAS simulated distributions of m_{12}, $\cos\theta_1'$, and $\cos\theta_2'$ the bin sums are also close to 41. We take $N_{4\ell}^{\rm ATLAS} = 45$ for all our distributions, and our bin sums $\Sigma_{m_{12}}$, $\Sigma_{\cos\theta_1'}$, and Σ_ϕ are significantly closer to 45 than those for the ATLAS simulated distributions.

On the other hand, the ATLAS simulations take into account that for the 45 measured decays $m_{4\ell}$ varies from 115 GeV to 130 GeV while we use Eqs. (A1) and (A2), which are derived for the case $m_{4\ell} = m_h$.

Summarizing the comparison with the ATLAS results, we note that our distributions are derived by integration of analytical formulas obtained for $m_{4\ell} = m_h$ and we have thoroughly chosen the total number of decays. ATLAS has used MC simulations and has accounted for the fact that for the measured decays $m_{4\ell}$ varies from 115 GeV to 130 GeV. Both techniques have advantages and disadvantages, and therefore it is not surprising that the ATLAS simulated distributions and our distributions somewhat differ but are equally close to the ATLAS experimental

Table IV: The sums over all the bins for each plot in Fig. 5 ($\Sigma_{m_{12}}$, $\Sigma_{m_{34}}$,$\Sigma_{\cos\theta_1'}$, $\Sigma_{\cos\theta_2'}$, and Σ_ϕ) for the ATLAS experimental data, for the ATLAS MC simulated distributions, and for our distributions.

	ATLAS exp. data	ATLAS MC simulated distributions	Our distributions
$\Sigma_{m_{12}}$	45	40.31	46.16
$\Sigma_{m_{34}}$	41	41.14	43.31
$\Sigma_{\cos\theta_1'}$	45	40.81	47.24
$\Sigma_{\cos\theta_2'}$	n/a	n/a	46.63
Σ_ϕ	45	41.09	46.30

distributions (see Fig. 5). In addition, we present our distribution of $\cos\theta_2'$.

In Ref. [6] CMS reports about 50 observed decays $h \to VV \to 4\ell$ with $m_{4\ell} \in (105.6\,\text{GeV}, 140.6\,\text{GeV})$ (see Table 3 there). textcolorredIn view of this, in order to calculate distributions for the CMS limitations (18), we choose $N_{4\ell}^{\text{CMS}} = 50$ in Eq. (D10). The accuracy of our distributions shown in Fig. 6 can be characterized by the sums over all the bins for each plot (see Table V). The plots in Fig. 6 are smoother than those in Fig. 5 due to their smaller bin widths.

Table V: The sums over all the bins for each plot in Fig. 6.

	Our distributions
$\Sigma_{m_{12}}$	51.30
$\Sigma_{m_{34}}$	55.91
$\Sigma_{\cos\theta_1'}$	52.14
$\Sigma_{\cos\theta_2'}$	52.03
Σ_ϕ	51.34

V. CONCLUSIONS

In this paper, we have considered the decay of a neutral particle X with zero spin and arbitrary CP parity into two off-mass-shell Z bosons (Z_1^* and Z_2^*) each of which decays to identical fermion-antifermion pairs ($f\bar{f}$): $X \to Z_1^* Z_2^* \to f\bar{f}f\bar{f}$. Analytical formulas for the fully differential width of the decay in question and for the fully differential width of the decay $h \to Z_1^* Z_2^* \to 4\ell$ are derived (see Eqs. (A1) and (D8)). Moreover, we present an exact formula for the differential width $\frac{d\Gamma}{da}$ of a decay $X \to Z_1^* Z_2^* \to f_1\bar{f}_1 f_2\bar{f}_2$ with $f_1 \neq f_2$ (see Eq. (B2)).

Integrating Eq. (A1) with a MC method, we have obtained some non-histogram distributions for any decay $h \to Z_1^* Z_2^* \to l_1^- l_1^+ l_2^- l_2^+$ ($l_j = e, \mu, \tau$) with $l_1 = l_2$. These distributions are compared to those for the decay $h \to Z_1^* Z_2^* \to l_1^- l_1^+ l_2^- l_2^+$ with $l_1 \neq l_2$ (see Figs. 3 and 4). The comparison has revealed significant distinctions between the distributions for the case $l_1 = l_2$ and the corresponding ones for $l_1 \neq l_2$. The dependences shown in

Fig. 4 are calculated at 4 possible sets (14) of values of the hZZ couplings a_Z, b_Z, and c_Z. At all the 4 sets these distributions almost coincide. Therefore their measurement can yield notable constraints on a_Z, b_Z, and c_Z only if the distributions are measured at very high precision.

In order to determine the usefulness of Eq. (A1), we have computed some SM histogram distributions of the decay $h \to Z_1^* Z_2^* \to 4\ell$ by means of integration of Eq. (D10). The distributions are calculated for ATLAS kinematical limitations (16) and for CMS ones (18).

We have compared our distributions with the ATLAS experimental ones and the ATLAS MC simulated ones (see Ref. [5]). The way our distributions are derived is almost purely analytical — its only numerical part is integration of Eq. (D10). Besides, we have chosen the total number of decays more accurately than ATLAS during its simulations. However, our calculation does not allow for the fact that the invariant mass of 4ℓ may differ from m_h while this fact is taken into account in the ATLAS simulations. The pros and cons of our technique and the ATLAS simulations make our distributions and the ATLAS simulated ones somewhat different but equally close to the ATLAS experimental data.

We have also presented our distributions of m_{12}, m_{34}, $\cos\theta_1'$, $\cos\theta_2'$, and ϕ for the kinematic conditions specific for CMS.

In summary, various distributions of the decays $X \to Z_1^* Z_2^* \to f\bar{f}f\bar{f}$ or $h \to Z_1^* Z_2^* \to 4\ell$ have been obtained with a rather simple integration of Eqs. (A1) and (D8) respectively. This way of calculation gives an alternative to more traditional MC simulation.

Acknowledgments

This research is partially supported by the National Academy of Sciences of Ukraine (project TsO-1-4/2017) and the Ministry of Education and Science of Ukraine (project no. 0115U000473 and project "Electromagnetic processes and processes involving short-lived particles in crystals at energies attainable at CERN").

Appendix A: The fully differential width of the decay $X \to Z_1^* Z_2^* \to f\bar{f}f\bar{f}$

The fully differential width of decay (3) is

$$\begin{aligned}
\frac{d^5\Gamma}{da_1 da_2 d\theta_1 d\theta_2 d\varphi} =& \frac{1}{4}\Bigg[\frac{d^5\Gamma_{f_1\neq f_2}}{da_1 da_2 d\theta_1 d\theta_2 d\varphi}\Big|_{f_1=f_2=f} + \frac{\sqrt{2}G_F^3 m_Z^8}{(4\pi)^6 m_X^3} \frac{k\sqrt{\tilde{a}_1\tilde{a}_2}}{D(\tilde{a}_1)D(\tilde{a}_2)} (a_f^2+v_f^2)^2 \sin\theta_1 \sin\theta_2 \\
&\times \Bigg\{ \sqrt{\tilde{a}_1\tilde{a}_2}\Big\{ \big((1+\bar{\alpha}_3^2)(1+\bar{\beta}_3^2) + 4A_f^2\bar{\alpha}_3\bar{\beta}_3\big)\left(|\tilde{A}_\parallel|^2 + |\tilde{A}_\perp|^2\right) + 4(1-\bar{\alpha}_3^2)(1-\bar{\beta}_3^2)|\tilde{A}_0|^2 \\
&- 4A_f\left(\bar{\alpha}_3(1+\bar{\beta}_3^2) + \bar{\beta}_3(1+\bar{\alpha}_3^2)\right)\mathrm{Re}(\tilde{A}_\parallel^*\tilde{A}_\perp) + 4\sqrt{2}\Big((A_f^2+\bar{\alpha}_3\bar{\beta}_3)\big(\mathrm{Re}\eta_-\mathrm{Re}(\tilde{A}_0^*\tilde{A}_\parallel) \\
&+ \mathrm{Im}\eta_-\mathrm{Im}(\tilde{A}_0^*\tilde{A}_\perp)\big) - A_f(\bar{\alpha}_3+\bar{\beta}_3)\big(\mathrm{Re}\eta_-\mathrm{Re}(\tilde{A}_0^*\tilde{A}_\perp) + \mathrm{Im}\eta_-\mathrm{Im}(\tilde{A}_0^*\tilde{A}_\parallel)\big)\Big) \\
&+ \mathrm{Re}\eta_-^2(|\tilde{A}_\parallel|^2 - |\tilde{A}_\perp|^2) + 2\,\mathrm{Im}\eta_-^2\mathrm{Im}(\tilde{A}_\parallel^*\tilde{A}_\perp)\Big\} - \frac{\sqrt{a_1 a_2}}{D(a_1)D(a_2)} \\
&\times \mathrm{Re}\Big\{ (a_1 - m_Z^2 + im_Z\Gamma_Z)(a_2 - m_Z^2 + im_Z\Gamma_Z)(\tilde{a}_1 - m_Z^2 - im_Z\Gamma_Z)(\tilde{a}_2 - m_Z^2 - im_Z\Gamma_Z) \\
&\times \Big(\big((r_{\alpha\beta} + \frac{1}{r_{\alpha\beta}})(\mathrm{Re}\eta_-\tilde{A}_\parallel - i\mathrm{Im}\eta_-\tilde{A}_\perp) + 2\sqrt{2(1-\bar{\alpha}_3^2)(1-\bar{\beta}_3^2)}\tilde{A}_0\big) \\
&\times \big(((1+A_f^2)\cos\phi(1+\cos\theta_1\cos\theta_2) + i\cdot 2A_f\sin\phi(\cos\theta_1+\cos\theta_2))A_\parallel^* \\
&- (2A_f\cos\phi(\cos\theta_1+\cos\theta_2) + i(1+A_f^2)\sin\phi(1+\cos\theta_1\cos\theta_2))A_\perp^* \\
&+ \sqrt{2}(1+A_f^2)\sin\theta_1\sin\theta_2 A_0^*\big) + (r_{\alpha\beta} - \frac{1}{r_{\alpha\beta}})(i\mathrm{Im}\eta_-\tilde{A}_\parallel - \mathrm{Re}\eta_-\tilde{A}_\perp) \\
&\times \big((2A_f\cos\phi(1+\cos\theta_1\cos\theta_2) + i(1+A_f^2)\sin\phi(\cos\theta_1+\cos\theta_2))A_\parallel^* \\
&- ((1+A_f^2)\cos\phi(\cos\theta_1+\cos\theta_2) + i\cdot 2A_f\sin\phi(1+\cos\theta_1\cos\theta_2))A_\perp^* \\
&+ \sqrt{2}\cdot 2A_f\sin\theta_1\sin\theta_2 A_0^*\big)\Big)\Big\}\Bigg\}\Bigg], \qquad \text{(A1)}
\end{aligned}$$

where

$$\begin{aligned}
\frac{d^5\Gamma_{f_1\neq f_2}}{da_1 da_2 d\theta_1 d\theta_2 d\varphi} =& \frac{\sqrt{2}G_F^3 m_Z^8}{(4\pi)^6 m_X^3}(a_{f_1}^2+v_{f_1}^2)(a_{f_2}^2+v_{f_2}^2)\frac{k a_1 a_2}{D(a_1)D(a_2)} \\
&\times \sin\theta_1\sin\theta_2[(|A_\parallel|^2+|A_\perp|^2)\left((1+\cos^2\theta_1)(1+\cos^2\theta_2) + 4A_{f_1}A_{f_2}\cos\theta_1\cos\theta_2\right) \\
&+ 4|A_0|^2\sin^2\theta_1\sin^2\theta_2 - 4\,\mathrm{Re}(A_\parallel^* A_\perp)(A_{f_1}\cos\theta_1(1+\cos^2\theta_2) + A_{f_2}\cos\theta_2(1+\cos^2\theta_1)) \\
&+ 4\sqrt{2}\sin\theta_1\sin\theta_2((\mathrm{Re}(A_0^*A_\parallel)\cos\phi - \mathrm{Im}(A_0^*A_\perp)\sin\phi)(A_{f_1}A_{f_2} + \cos\theta_1\cos\theta_2) \\
&- (\mathrm{Re}(A_0^*A_\perp)\cos\phi - \mathrm{Im}(A_0^*A_\parallel)\sin\phi)(A_{f_1}\cos\theta_2 + A_{f_2}\cos\theta_1)) \\
&+ \sin^2\theta_1\sin^2\theta_2((|A_\parallel|^2 - |A_\perp|^2)\cos 2\phi - 2\,\mathrm{Im}(A_\parallel^* A_\perp)\sin 2\phi)] \qquad \text{(A2)}
\end{aligned}$$

is the fully differential width of decay (2) (see Eq. (5) in Ref. [7]), a_f is the weak isospin projection of the fermion f, $v_f \equiv a_f - 2\frac{q_f}{e}\sin^2\theta_W$, q_f is the electric charge of f, e is the electric charge of the positron, θ_W is the weak mixing angle, $D(x) \equiv (x - m_Z^2)^2 + (m_Z\Gamma_Z)^2$,

$$A_\pm \equiv \frac{A_{X\to Z_1^* Z_2^*}(p_1,p_2,\pm1,\pm1)}{g_Z}, \qquad A_0 \equiv \frac{A_{X\to Z_1^* Z_2^*}(p_1,p_2,0,0)}{g_Z}, \qquad \text{(A3)}$$

$$A_\parallel \equiv \frac{\tilde{A}_+ + \tilde{A}_-}{\sqrt{2}} = \sqrt{2}a_Z(a_1,a_2), \qquad A_\perp \equiv \frac{\tilde{A}_+ - \tilde{A}_-}{\sqrt{2}} = \sqrt{2}\frac{k}{m_X^2}c_Z(a_1,a_2), \qquad \text{(A4)}$$

$$A_f = \frac{2a_f v_f}{a_f^2 + v_f^2}, \tag{A5}$$

$\bar{\alpha}_i \equiv \frac{\alpha_i}{|\boldsymbol{\alpha}|}$ $(i = 1, 2, 3)$, $\boldsymbol{\alpha}$ is the momentum of the fermion f_1 in the center-of-momentum frame of the particles f_1 and $\bar{f}_2$,

$$\begin{aligned}
\boldsymbol{\alpha} =& \mathbf{e}_x \frac{\sqrt{a_1}(2E_2' + \sqrt{\tilde{a}_1})\sin\theta_1\cos\phi_1 + \sqrt{a_2}(2E_1 + \sqrt{\tilde{a}_1})\sin\theta_2\cos\phi_2}{4(E_1 + E_2' + \sqrt{\tilde{a}_1})} \\
&+ \mathbf{e}_y \frac{\sqrt{a_1}(2E_2' + \sqrt{\tilde{a}_1})\sin\theta_1\sin\phi_1 - \sqrt{a_2}(2E_1 + \sqrt{\tilde{a}_1})\sin\theta_2\sin\phi_2}{4(E_1 + E_2' + \sqrt{\tilde{a}_1})} + \frac{\bar{\mathbf{p}}_1}{8(E_1 + E_2' + \sqrt{\tilde{a}_1})} \\
&\times \Big((m_X^2 - a_1 - a_2)(\cos\theta_1 - \cos\theta_2) + k(1 - \cos\theta_1\cos\theta_2) \\
&+ \frac{\sqrt{\tilde{a}_1}}{m_X}(2k + (m_X^2 + a_1 - a_2)\cos\theta_1 - (m_X^2 + a_2 - a_1)\cos\theta_2)\Big),
\end{aligned} \tag{A6}$$

$$|\boldsymbol{\alpha}| = \frac{\sqrt{\tilde{a}_1}}{2}, \tag{A7}$$

$\bar{\mathbf{p}}_1 \equiv \frac{\mathbf{p}_1}{|\mathbf{p}_1|}$, $\mathbf{e}_x$ and $\mathbf{e}_y$ are any unit and mutually orthogonal vectors such that $\mathbf{e}_x \times \mathbf{e}_y = \bar{\mathbf{p}}_1$,

$$\begin{aligned}
E_1 \equiv k_1^0 &= \frac{m_X^2 + a_1 - a_2 + k\cos\theta_1}{4m_X}, \qquad E_1' \equiv k_1'^0 = \frac{m_X^2 + a_1 - a_2 - k\cos\theta_1}{4m_X} \\
E_2 \equiv k_2^0 &= \frac{m_X^2 + a_2 - a_1 + k\cos\theta_2}{4m_X}, \qquad E_2' \equiv k_2'^0 = \frac{m_X^2 + a_2 - a_1 - k\cos\theta_2}{4m_X},
\end{aligned} \tag{A8}$$

ϕ_1 is the azimuthal angle of the f_1 momentum in the Z_1^* rest frame formed by the vectors ($\mathbf{e}_x$, $\mathbf{e}_y$, $\bar{\mathbf{p}}_1$), ϕ_2 is the azimuthal angle of the f_2 momentum in the Z_2^* rest frame formed by the vectors ($\mathbf{e}_x$, $-\mathbf{e}_y$, $-\bar{\mathbf{p}}_1$),

$$\alpha_1 \equiv \boldsymbol{\alpha}\cdot\mathbf{e}_x, \quad \alpha_2 \equiv \boldsymbol{\alpha}\cdot\mathbf{e}_y, \quad \alpha_3 \equiv \boldsymbol{\alpha}\cdot\bar{\mathbf{p}}_1, \tag{A9}$$

$\bar{\beta}_i \equiv \frac{\beta_i}{|\boldsymbol{\beta}|}$ $(i = 1, 2, 3)$, $\boldsymbol{\beta}$ is the momentum of the fermion f_2 in the center-of-momentum frame of the particles f_2 and $\bar{f}_1$,

$$\begin{aligned}
\boldsymbol{\beta} &= \boldsymbol{\alpha}|_{\substack{a_1\leftrightarrow a_2,\theta_1\leftrightarrow\theta_2,\phi_1\leftrightarrow\phi_2 \\ \mathbf{e}_y\to-\mathbf{e}_y,\bar{\mathbf{p}}_1\to-\bar{\mathbf{p}}_1}} = \boldsymbol{\alpha}|_{k\to-k} \\
&= \mathbf{e}_x \frac{\sqrt{a_1}(2E_2 + \sqrt{\tilde{a}_2})\sin\theta_1\cos\phi_1 + \sqrt{a_2}(2E_1' + \sqrt{\tilde{a}_2})\sin\theta_2\cos\phi_2}{4(E_2 + E_1' + \sqrt{\tilde{a}_2})} \\
&+ \mathbf{e}_y \frac{\sqrt{a_1}(2E_2 + \sqrt{\tilde{a}_2})\sin\theta_1\sin\phi_1 - \sqrt{a_2}(2E_1' + \sqrt{\tilde{a}_2})\sin\theta_2\sin\phi_2}{4(E_2 + E_1' + \sqrt{\tilde{a}_2})} + \frac{\bar{\mathbf{p}}_1}{8(E_2 + E_1' + \sqrt{\tilde{a}_2})} \\
&\times \Big((m_X^2 - a_1 - a_2)(\cos\theta_1 - \cos\theta_2) - k(1 - \cos\theta_1\cos\theta_2) \\
&+ \frac{\sqrt{\tilde{a}_2}}{m_X}(-2k + (m_X^2 + a_1 - a_2)\cos\theta_1 - (m_X^2 + a_2 - a_1)\cos\theta_2)\Big),
\end{aligned} \tag{A10}$$

$$|\boldsymbol{\beta}| = \frac{\sqrt{\tilde{a}_2}}{2}, \tag{A11}$$

$$\beta_1 \equiv \boldsymbol{\beta}\cdot\mathbf{e}_x, \quad \beta_2 \equiv \boldsymbol{\beta}\cdot(-\mathbf{e}_y), \quad \beta_3 \equiv \boldsymbol{\beta}\cdot(-\bar{\mathbf{p}}_1), \tag{A12}$$

$$\tilde{A}_\pm \equiv \frac{A_{X\to Z_1^* Z_2^*}(\tilde{p}_1, \tilde{p}_2, \pm 1, \pm 1)}{g_Z}, \qquad \tilde{A}_0 \equiv \frac{A_{X\to Z_1^* Z_2^*}(\tilde{p}_1, \tilde{p}_2, 0, 0)}{g_Z}, \tag{A13}$$

$$\tilde{A}_\parallel \equiv \frac{\tilde{A}_+ + \tilde{A}_-}{\sqrt{2}} = \sqrt{2}a_Z(\tilde{a}_1, \tilde{a}_2), \qquad \tilde{A}_\perp \equiv \frac{\tilde{A}_+ - \tilde{A}_-}{\sqrt{2}} = \frac{2\sqrt{2}}{m_X}|\mathbf{k}_1 + \mathbf{k}_2'|c_Z(\tilde{a}_1, \tilde{a}_2), \tag{A14}$$

$$\eta_- \equiv (\bar\alpha_1 - i\bar\alpha_2)(\bar\beta_1 - i\bar\beta_2)$$
$$= \frac{1}{4\sqrt{\tilde a_1\tilde a_2}(E_1+E_2'+\sqrt{\tilde a_1})(E_2+E_1'+\sqrt{\tilde a_2})}\Bigg(a_1(2E_2+\sqrt{\tilde a_2})(2E_2'+\sqrt{\tilde a_1})\sin^2\theta_1$$
$$+ a_2(2E_1'+\sqrt{\tilde a_2})(2E_1+\sqrt{\tilde a_1})\sin^2\theta_2 + \sqrt{a_1a_2}\sin\theta_1\sin\theta_2\Big((2E_2'+\sqrt{\tilde a_1})(2E_1'+\sqrt{\tilde a_2})e^{-i\phi}$$
$$+ (2E_1+\sqrt{\tilde a_1})(2E_2+\sqrt{\tilde a_2})e^{i\phi}\Big)\Bigg), \tag{A15}$$

$$r_{\alpha\beta} \equiv \sqrt{\frac{(1+\bar\alpha_3)(1+\bar\beta_3)}{(1-\bar\alpha_3)(1-\bar\beta_3)}}. \tag{A16}$$

Note that the dependence of expression (A1) on ϕ_1 and ϕ_2 reduces to a dependence on $\phi_1+\phi_2$ and in Eq. (A1) the latter sum has to be substituted by ϕ.

Appendix B: $\frac{d\Gamma}{da}$ of a decay $X \to Z_1^* Z_2^* \to f_1\bar f_1 f_2\bar f_2$ with $f_1 \neq f_2$

It follows from Eq. (C9) that for any decay (2)

$$\frac{d\Gamma}{da} = \frac{d\Gamma}{da_2}\bigg|_{a_2=a} = \left(\int_0^{(m_X-\sqrt{a_2})^2} da_1 \frac{d^2\Gamma}{da_1 da_2}\right)\bigg|_{a_2=a}, \tag{B1}$$

where the differential width $\frac{d^2\Gamma}{da_1 da_2}$ is determined by Eq. (8) from Ref. [7].

If the functions $|a_Z(a_1,a_2)|$, $|b_Z(a_1,a_2)|$, $|c_Z(a_1,a_2)|$, and $\mathrm{Re}(a_Z^*(a_1,a_2)\,b_Z(a_1,a_2))$ are independent of a_1 and a_2,

integration of $\frac{d^2\Gamma}{da_1 da_2}$ in Eq. (B1) yields

$$\begin{aligned}
\frac{d\Gamma}{da} =& \frac{\sqrt{2}G_F^3 m_Z^8 m_X}{2^{11}3^3\pi^5}(a_{f_1}^2+v_{f_1}^2)(a_{f_2}^2+v_{f_2}^2)\frac{1}{D(a)} \\
&\times\Bigg[(1-\alpha)\Big\{24(-23\alpha+4\eta+1)|a_Z|^2-16(2\alpha^2+(9\eta+17)\alpha+3\beta^2-9\eta^2-3\eta \\
&-1)\mathrm{Re}(a_Z^* b_Z)+(3\alpha^3+(8\eta-45)\alpha^2+(18\eta^2-208\eta-45)\alpha-6(8\eta+1)\beta^2-6\alpha\beta^2+48\eta^3 \\
&+18\eta^2+8\eta+3)|b_Z|^2+64\alpha(\alpha^2+2(3\eta+17)\alpha+6\beta^2-18\eta^2+6\eta+1)|c_Z|^2\Big\} \\
&+6\ln\left(\frac{1}{\alpha}\right)\Big\{4(12\alpha^2+6(1-4\eta)\alpha-\beta^2+3\eta^2)|a_Z|^2+8(6\alpha^2-3\eta(\eta+2)\alpha \\
&+\alpha\beta^2-2\eta\beta^2+2\eta^3)\mathrm{Re}(a_Z^* b_Z)+(30\alpha^2+\beta^4+10\alpha\beta^2-30\eta^2\alpha-10\eta^2\beta^2+5\eta^4)|b_Z|^2+32\alpha \\
&\times(-6\alpha^2+3(\eta^2+4\eta-2)\alpha+(4\eta-1)\beta^2-\alpha\beta^2+\eta^2(3-4\eta))|c_Z|^2\Big\}+s\cdot 3\sqrt{2} \\
&\times\Big\{\left(\frac{1}{\beta}P_1 r_{+\eta}-4P_2 r_{-\eta}\right)\ln\Big(\frac{1}{4\alpha(\frac{m_Z^4}{m_X^4}+\beta^2)} \\
&\times(\alpha^2\beta^2+(\eta-4)^2\alpha^2+2\alpha\beta^2+2\eta(\eta-4)\alpha+\beta^2+\eta^2-s\sqrt{2}(1-\alpha) \\
&\times(\beta(\alpha+1)r_{+\eta}+((\eta-4)\alpha+\eta)r_{-\eta})+(1-\alpha)^2\sqrt{(4\alpha+\beta^2-\eta^2)^2+4\eta^2\beta^2})\Big) \\
&+2\left(4P_2 r_{+\eta}+\frac{1}{\beta}P_1 r_{-\eta}\right)(\pi-\arg((\eta-4)\alpha^2+(-\eta^2+6\eta-4)\alpha-\alpha\beta^2-\beta^2 \\
&+\eta(1-\eta)+s\frac{1-\alpha}{\sqrt{2}}(\beta r_{+\eta}-\frac{m_Z^2}{m_X^2}r_{-\eta})+i(1-\alpha)(-\beta(1-\alpha) \\
&+s\frac{\frac{m_Z^2}{m_X^2}r_{+\eta}+\beta r_{-\eta}}{\sqrt{2}})))\Big\}\Bigg],
\end{aligned} \tag{B2}$$

where $\alpha(a)\equiv\frac{a}{m_X^2}$, $\beta\equiv\frac{m_Z\Gamma_Z}{m_X^2}$, $\eta(a)\equiv 1+\frac{a-m_Z^2}{m_X^2}$, in place of s one may take either 1 or -1 (this choice does not influence the dependence of $\frac{d\Gamma}{da}$ on a),

$$\begin{aligned}
P_1 \equiv& 4(12\alpha^2+4(2-3\eta)\alpha-\beta^2+\eta^2)|a_Z|^2+4(8\alpha^2-2\eta(\eta+2)\alpha-3\eta\beta^2+2\alpha\beta^2+\eta^3)\mathrm{Re}(a_Z^* b_Z) \\
&+((4\alpha+\beta^2)^2+\eta^2(\eta^2-8\alpha-6\beta^2))|b_Z|^2-32\alpha(4\alpha^2+\alpha\beta^2+(4-4\eta-\eta^2)\alpha \\
&+(1-3\eta)\beta^2+\eta^2(\eta-1))|c_Z|^2, \\
P_2 \equiv& 2(6\alpha-\eta)|a_Z|^2+(4(\eta+1)\alpha+\beta^2-3\eta^2)\mathrm{Re}(a_Z^* b_Z)+\eta(4\alpha+\beta^2-\eta^2)|b_Z|^2 \\
&-8\alpha(2(\eta+2)\alpha+\beta^2+\eta(2-3\eta))|c_Z|^2, \\
r_{\pm\eta} \equiv& \sqrt{\sqrt{(4\alpha+\beta^2-\eta^2)^2+4\eta\beta^2}\pm(4\alpha+\beta^2-\eta^2)}.
\end{aligned} \tag{B3}$$

We define the argument $\arg z$ of a complex number z as follows:

$$\begin{aligned}
&\arg z = \arctan\frac{\mathrm{Im}\, z}{\mathrm{Re}\, z}+\pi n(\mathrm{Re}\, z,\,\mathrm{Im}\, z) \quad \forall z\in C|\mathrm{Re}\, z\neq 0, \\
&\arg z = \pi\left(\frac{1}{2}+\Theta(-\mathrm{Im}\, z)\right) \quad \forall z\in C|(\mathrm{Re}\, z=0 \ \text{ and } \ \mathrm{Im}\, z\neq 0),
\end{aligned} \tag{B4}$$

where $n(x,y)\equiv\Theta(-x)+2\,\Theta(x)\Theta(-y) \ \ \forall x\neq 0$,

$$\Theta(x)\equiv 0 \ \ \forall x\in(-\infty,0], \quad \Theta(x)\equiv 1 \ \ \forall x\in(0,+\infty). \tag{B5}$$

According to definition (B4), $\arg z \in [0, 2\pi)$.

Appendix C: The definitions and explicit formulas for $\frac{d\Gamma}{da}$ and $\frac{d\Gamma}{d\theta}$

In this Appendix we propose some general definitions of the differential widths $\frac{d\Gamma}{da}$ and $\frac{d\Gamma}{d\theta}$ for any decay (1), and show that the differential widths defined this way coincide with those defined in the standard fashion for decays (2) and (3) separately. Therefore, the distributions presented in Fig. 4a are general distributions defined for any decay (1) which are calculated for the decay into non-identical leptons and the distributions in Fig. 4b are the same general distributions calculated for the decay into identical leptons. Thus, comparison of Fig. 4a and Fig. 4b is sensible thanks to the existence of the general definitions of $\frac{d\Gamma}{da}$ and $\frac{d\Gamma}{d\theta}$.

1. The differential width $\frac{d\Gamma}{da}$

We define the function $\frac{d\Gamma}{da}$ as

$$\frac{1}{\Gamma}\frac{d\Gamma}{da} \equiv \frac{1}{2}\frac{dP_a}{da}, \tag{C1}$$

where dP_a is the probability that in decay (1) there is a Z boson whose squared invariant mass lies in an interval $[a, a + da]$. To derive an explicit formula for the distribution $\frac{1}{\Gamma}\frac{d\Gamma}{da}$, we should recall that for decay (2)

$$\lim_{N\to\infty} \frac{1}{N}\frac{d^5 N_{f_1\neq f_2}}{d^5 p} = \frac{1}{\Gamma}\frac{d^5\Gamma}{d^5 p}, \tag{C2}$$

where $d^5 p \equiv da_1 da_2 d\theta_1 d\theta_2 d\phi$, $d^5 N_{f_1\neq f_2}$ is the number of the decays (2) in which the squared invariant mass of Z_1^* (Z_2^*) is in an interval $[a_1, a_1 + da_1]$ ($[a_2, a_2 + da_2]$), the polar angle of f_1 (f_2) lies in $[\theta_1, \theta_1 + d\theta_1]$ ($[\theta_2, \theta_2 + d\theta_2]$), and the azimuthal angle between the planes of the decays $Z_1^* \to f_1\bar{f}_1$ and $Z_2^* \to f_2\bar{f}_2$ is in an interval $[\phi, \phi + d\phi]$, among N decays (2).

Eq. (C2) is consistent with the fact that for any decay (1)

$$\int\limits_0^{m_X^2} da_1 \int\limits_0^{(m_X-\sqrt{a_1})^2} da_2 \int\limits_0^{\pi} d\theta_1 \int\limits_0^{\pi} d\theta_2 \int\limits_0^{2\pi} d\phi \frac{d^5\Gamma}{d^5 p} = \Gamma, \tag{C3}$$

because

$$\int\limits_0^{m_X^2} da_1 \int\limits_0^{(m_X-\sqrt{a_1})^2} da_2 \int\limits_0^{\pi} d\theta_1 \int\limits_0^{\pi} d\theta_2 \int\limits_0^{2\pi} d\phi \frac{d^5 N_{f_1\neq f_2}}{d^5 p} = N. \tag{C4}$$

Using Eqs. (C1) and (C2), we obtain that for decay (2)

$$\begin{aligned}\frac{1}{\Gamma}\frac{d\Gamma}{da} &= \frac{1}{2}\lim_{N\to\infty}\frac{1}{N}\left(\left.\frac{dN_{f_1\neq f_2}}{da_1}\right|_{a_1=a} + \left.\frac{dN_{f_1\neq f_2}}{da_2}\right|_{a_2=a}\right) = \frac{1}{2}\left(\left.\frac{1}{\Gamma}\frac{d\Gamma}{da_1}\right|_{a_1=a} + \left.\frac{1}{\Gamma}\frac{d\Gamma}{da_2}\right|_{a_2=a}\right) \\ &= \left.\frac{1}{\Gamma}\frac{d\Gamma}{da_1}\right|_{a_1=a} = \left.\frac{1}{\Gamma}\frac{d\Gamma}{da_2}\right|_{a_2=a},\end{aligned} \tag{C5}$$

since if we neglect m_{f_1} and m_{f_2}, then $\frac{d\Gamma}{da_1}\Big|_{a_1=a} = \frac{d\Gamma}{da_2}\Big|_{a_2=a}$ (see Eq. (8) in Ref. [7]).

For any decay (3)

$$\lim_{N\to\infty}\frac{1}{N}\frac{d^5N_{f_1=f_2}}{d^5p} = \frac{1}{\Gamma}\cdot 2\frac{d^5\Gamma}{d^5p}, \tag{C6}$$

where $d^5N_{f_1=f_2}$ is the number of the decays (3) in which there is a Z boson Z_1^* with a squared invariant mass lying in an interval $[a_1, a_1+da_1]$ and a Z boson Z_2^* whose squared invariant mass is in $[a_2, a_2+da_2]$, the polar angle of f_1 (f_2) lies in an interval $[\theta_1, \theta_1+d\theta_1]$ ($[\theta_2, \theta_2+d\theta_2]$), and the azimuthal angle between the planes of the decays $Z_1^*\to f_1\bar{f}_1$ and $Z_2^*\to f_2\bar{f}_2$ is in $[\phi, \phi+d\phi]$, among N decays (3). Note that while for decay (2) Z_1^* (Z_2^*) is defined as the Z boson decaying into $f_1\bar{f}_1$ ($f_2\bar{f}_2$), for decay (3) the choice of Z_1^* and Z_2^* is arbitrary, which leads to the difference between the definitions of $d^5N_{f_1\neq f_2}$ and $d^5N_{f_1=f_2}$.

Eq. (C6) accords with Eq. (C3) due to the fact that

$$\int\limits_0^{m_X^2} da_1 \int\limits_0^{(m_X-\sqrt{a_1})^2} da_2 \int\limits_0^{\pi} d\theta_1 \int\limits_0^{\pi} d\theta_2 \int\limits_0^{2\pi} d\phi \frac{d^5N_{f_1=f_2}}{d^5p} = 2N. \tag{C7}$$

The "2" in the right-hand side of Eq. (C7) emerges because of the double counting during the integration of $\frac{d^5N_{f_1=f_2}}{d^5p}$ on a_1 and a_2.

It follows from Eqs. (C1) and (C6) that for decay (3)

$$\frac{1}{\Gamma}\frac{d\Gamma}{da} = \frac{1}{2}\lim_{N\to\infty}\frac{1}{N}\frac{dN_{f_1=f_2}}{da_1}\Big|_{a_1=a} = \frac{1}{2}\lim_{N\to\infty}\frac{1}{N}\frac{dN_{f_1=f_2}}{da_2}\Big|_{a_2=a} = \frac{1}{\Gamma}\frac{d\Gamma}{da_1}\Big|_{a_1=a} = \frac{1}{\Gamma}\frac{d\Gamma}{da_2}\Big|_{a_2=a}. \tag{C8}$$

Combining Eqs. (C5) and (C8), we infer that in the approximation $m_{f_1} = m_{f_2} = 0$ for any decay (1)

$$\frac{d\Gamma}{da} = \frac{d\Gamma}{da_1}\Big|_{a_1=a} = \frac{d\Gamma}{da_2}\Big|_{a_2=a}. \tag{C9}$$

2. The differential width $\frac{d\Gamma}{d\theta}$

Analogously, we define the differential width $\frac{d\Gamma}{d\theta}$ as

$$\frac{1}{\Gamma}\frac{d\Gamma}{d\theta} \equiv \frac{1}{2}\frac{dP_\theta}{d\theta}, \tag{C10}$$

where dP_θ is the probability that in decay (1) there is a fermion whose polar angle lies in an interval $[\theta, \theta+d\theta]$.

Eqs. (C10) and (C2) yield that for any decay (2)

$$\frac{1}{\Gamma}\frac{d\Gamma}{d\theta} = \frac{1}{2}\lim_{N\to\infty}\frac{1}{N}\left(\frac{dN_{f_1\neq f_2}}{d\theta_1}\Big|_{\theta_1=\theta} + \frac{dN_{f_1\neq f_2}}{d\theta_2}\Big|_{\theta_2=\theta}\right) = \frac{1}{2}\left(\frac{1}{\Gamma}\frac{d\Gamma}{d\theta_1}\Big|_{\theta_1=\theta} + \frac{1}{\Gamma}\frac{d\Gamma}{d\theta_2}\Big|_{\theta_2=\theta}\right). \tag{C11}$$

According to Eq. (A2), the differential width $\frac{d^2\Gamma}{d\theta_1 d\theta_2}$ of decay (2) is invariant under the substitution $\theta_1\to\theta_2$ and $\theta_2\to\theta_1$ if $A_{f_1} = A_{f_2}$ (see Eq. (A5) for the definition of the quantity A_f). That is why for decay (2) in the case $A_{f_1} = A_{f_2}$

$$\frac{d\Gamma}{d\theta_1}\Big|_{\theta_1=\theta} = \frac{d\Gamma}{d\theta_2}\Big|_{\theta_2=\theta}, \tag{C12}$$

and therefore

$$\frac{1}{\Gamma}\frac{d\Gamma}{d\theta} = \frac{1}{\Gamma}\frac{d\Gamma}{d\theta_1}\bigg|_{\theta_1=\theta} = \frac{1}{\Gamma}\frac{d\Gamma}{d\theta_2}\bigg|_{\theta_2=\theta}. \tag{C13}$$

We find from Eqs. (C10) and (C6) that for decay (3)

$$\frac{1}{\Gamma}\frac{d\Gamma}{d\theta} = \frac{1}{2}\lim_{N\to\infty}\frac{1}{N}\frac{dN_{f_1=f_2}}{d\theta_1}\bigg|_{\theta_1=\theta} = \frac{1}{2}\lim_{N\to\infty}\frac{1}{N}\frac{dN_{f_1=f_2}}{d\theta_2}\bigg|_{\theta_2=\theta} = \frac{1}{\Gamma}\frac{d\Gamma}{d\theta_1}\bigg|_{\theta_1=\theta} = \frac{1}{\Gamma}\frac{d\Gamma}{d\theta_2}\bigg|_{\theta_2=\theta}. \tag{C14}$$

Combination of Eqs. (C13) and (C14) yields that for any decay (1) wherein $A_{f_1} = A_{f_2}$

$$\frac{d\Gamma}{d\theta} = \frac{d\Gamma}{d\theta_1}\bigg|_{\theta_1=\theta} = \frac{d\Gamma}{d\theta_2}\bigg|_{\theta_2=\theta}. \tag{C15}$$

Appendix D: The fully differential distribution of the decay $h \to Z_1^* Z_2^* \to 4\ell$

It follows from Eqs. (C6), (C2), (16), and (18) that

$$\lim_{N_k\to\infty}\frac{N_k^i}{N_k} = \frac{\Gamma_k^i}{\Gamma_k}, \qquad k = 4e, 4\mu, 2e2\mu, \qquad i = \text{ATLAS, CMS}, \tag{D1}$$

where N_k^i is the number of the decays $h \to Z_1^* Z_2^* \to k$ selected by ATLAS or CMS, among N_k decays $h \to Z_1^* Z_2^* \to k$,

$$\Gamma_k \equiv \int\limits_0^{m_X^2} da_1 \int\limits_0^{a_{2\,max}} da_2 \int\limits_0^{\pi} d\theta_1 \int\limits_0^{\pi} d\theta_2 \int\limits_0^{2\pi} d\phi\, 2\frac{d^5\Gamma_k}{d^5 p}, \tag{D2}$$

$a_{2\,max} \equiv \text{Min}\left(a_1, (m_X - \sqrt{a_1})^2\right)$, $\frac{d^5\Gamma_k}{d^5 p}$ is the fully differential width of the decay $h \to Z_1^* Z_2^* \to k$ (see Eqs. (A1) and (A2)),

$$\begin{aligned}
\Gamma_{4e}^i &\equiv \int\limits_{a_{1\,min}^i}^{a_{1\,max}^i} da_1 \int\limits_{a_{2\,min}^i}^{a_{2\,max}} da_2 \int\limits_{\theta_{e\,min}^i}^{\pi-\theta_{e\,min}^i} d\theta_1 \int\limits_{\theta_{e\,min}^i}^{\pi-\theta_{e\,min}^i} d\theta_2 \int\limits_0^{2\pi} d\phi\, 2\frac{d^5\Gamma_{4e}}{d^5 p},\\
\Gamma_{4\mu}^i &\equiv \int\limits_{a_{1\,min}^i}^{a_{1\,max}^i} da_1 \int\limits_{a_{2\,min}^i}^{a_{2\,max}} da_2 \int\limits_{\theta_{\mu\,min}^i}^{\pi-\theta_{\mu\,min}^i} d\theta_1 \int\limits_{\theta_{\mu\,min}^i}^{\pi-\theta_{\mu\,min}^i} d\theta_2 \int\limits_0^{2\pi} d\phi\, 2\frac{d^5\Gamma_{4\mu}}{d^5 p},\\
\Gamma_{2e2\mu}^i &\equiv \int\limits_{a_{1\,min}^i}^{a_{1\,max}^i} da_1 \int\limits_{a_{2\,min}^i}^{a_{2\,max}} da_2 \int\limits_{\theta_{e\,min}^i}^{\pi-\theta_{e\,min}^i} d\theta_1 \int\limits_{\theta_{\mu\,min}^i}^{\pi-\theta_{\mu\,min}^i} d\theta_2 \int\limits_0^{2\pi} d\phi\, 2\frac{d^5\Gamma_{2e2\mu}}{d^5 p},
\end{aligned} \tag{D3}$$

$$\begin{aligned}
&a_{1\,min}^{\text{ATLAS}} = (50\,\text{GeV})^2, \qquad a_{1\,max}^{\text{ATLAS}} = (106\,\text{GeV})^2, \qquad a_{2\,min}^{\text{ATLAS}} = (12\,\text{GeV})^2,\\
&\theta_{e\,min}^{\text{ATLAS}} \equiv 2\arctan e^{-2.47}, \qquad \theta_{\mu\,min}^{\text{ATLAS}} \equiv 2\arctan e^{-2.7},
\end{aligned} \tag{D4}$$

$$\begin{aligned}
&a_{1\,min}^{\text{CMS}} = (40\,\text{GeV})^2, \qquad a_{1\,max}^{\text{CMS}} = (m_X - 12\,\text{GeV})^2, \qquad a_{2\,min}^{\text{CMS}} = (12\,\text{GeV})^2,\\
&\theta_{e\,min}^{\text{CMS}} \equiv 2\arctan e^{-2.5}, \qquad \theta_{\mu\,min}^{\text{CMS}} \equiv 2\arctan e^{-2.4}.
\end{aligned} \tag{D5}$$

Moreover, the fully differential distribution of the decay $h \to Z_1^* Z_2^* \to 4\ell$ is

$$\lim_{N_{4\ell}\to\infty} \frac{1}{N_{4\ell}} \frac{d^5 N_{4\ell}}{d^5 p} = \lim_{N_{4\ell}\to\infty} \frac{1}{N_{4e} + N_{4\mu} + N_{2e2\mu}} \frac{d^5 N_{4e} + d^5 N_{4\mu} + d^5 N'_{2e2\mu}}{d^5 p}$$
$$= \lim_{N_{4\ell}\to\infty} \frac{1}{2N_{4e} + N_{2e2\mu}} \frac{2d^5 N_{4e} + d^5 N'_{2e2\mu}}{d^5 p}, \tag{D6}$$

where

- $d^5 N_{4\ell}$ is the number of the decays $h \to Z_1^* Z_2^* \to 4\ell$ in which $m_{12}^2 \in [a_1, a_1 + da_1]$, $m_{34}^2 \in [a_2, a_2 + da_2]$, the polar angle of f_1 (f_2) lies in an interval $[\theta_1, \theta_1 + d\theta_1]$ ($[\theta_2, \theta_2 + d\theta_2]$), and the azimuthal angle between the planes of the decays $Z_1^* \to f_1 \bar{f}_1$ and $Z_2^* \to f_2 \bar{f}_2$ is in $[\phi, \phi + d\phi]$, among $N_{4\ell}$ decays $h \to Z_1^* Z_2^* \to 4\ell$;

- $d^5 N'_{2e2\mu}$ is the number of the decays $h \to Z_1^* Z_2^* \to 2e2\mu$ in which $m_{12}^2 \in [a_1, a_1 + da_1]$, $m_{34}^2 \in [a_2, a_2 + da_2]$, the polar angle of f_1 (f_2) lies in an interval $[\theta_1, \theta_1 + d\theta_1]$ ($[\theta_2, \theta_2 + d\theta_2]$), and the azimuthal angle between the planes of the decays $Z_1^* \to f_1 \bar{f}_1$ and $Z_2^* \to f_2 \bar{f}_2$ is in $[\phi, \phi + d\phi]$, among $N_{4\ell}$ decays $h \to Z_1^* Z_2^* \to 4\ell$.

Hereinafter, the symbol Z_1^* (Z_2^*) denotes the Z boson whose mass is m_{12} (m_{34}) and f_1 (f_2) denotes the fermion whose parent Z boson is Z_1^* (Z_2^*).

It follows from Eqs. (C2) and (A2) that

$$d^5 N'_{2e2\mu} = 2\, d^5 N_{2e2\mu}. \tag{D7}$$

Using Eqs. (D6) and (D7), we derive that

$$\lim_{N_{4\ell}\to\infty} \frac{1}{N_{4\ell}} \frac{d^5 N_{4\ell}}{d^5 p} = \lim_{N_{4\ell}\to\infty} \frac{2}{2\Gamma_{4e} + \Gamma_{2e2\mu}} \left(\frac{\Gamma_{4e}}{N_{4e}} \frac{d^5 N_{4e}}{d^5 p} + \frac{\Gamma_{2e2\mu}}{N_{2e2\mu}} \frac{d^5 N_{2e2\mu}}{d^5 p} \right)$$
$$= \frac{2}{2\Gamma_{4e} + \Gamma_{2e2\mu}} \left(2\frac{d^5 \Gamma_{4e}}{d^5 p} + \frac{d^5 \Gamma_{2e2\mu}}{d^5 p} \right), \tag{D8}$$

Integration of Eq. (D8) yields

$$\lim_{N_{4\ell}\to\infty} \frac{N^i_{4\ell}}{N_{4\ell}} = \frac{2\Gamma^i_{4e} + \Gamma^i_{2e2\mu}}{2\Gamma_{4e} + \Gamma_{2e2\mu}}, \tag{D9}$$

where $N^i_{4\ell}$ is the number of the decays $h \to Z_1^* Z_2^* \to 4\ell$ selected by ATLAS or CMS, among $N_{4\ell}$ decays $h \to Z_1^* Z_2^* \to 4\ell$.

Besides, we obtain from Eq. (D8) that

$$\lim_{N_{4\ell}\to\infty} \frac{1}{N^i_{4\ell}} \frac{d^5 N_{4\ell}}{d^5 p} = \frac{2}{2\Gamma_{4e} + \Gamma_{2e2\mu}} \left(2\frac{d^5 \Gamma_{4e}}{d^5 p} + \frac{d^5 \Gamma_{2e2\mu}}{d^5 p} \right) \lim_{N_{4\ell}\to\infty} \frac{N_{4e} + N_{4\mu} + N_{2e2\mu}}{N^i_{4e} + N^i_{4\mu} + N^i_{2e2\mu}}$$
$$= \frac{2}{\Gamma^i_{4e} + \Gamma^i_{4\mu} + \Gamma^i_{2e2\mu}} \left(2\frac{d^5 \Gamma_{4e}}{d^5 p} + \frac{d^5 \Gamma_{2e2\mu}}{d^5 p} \right). \tag{D10}$$

[1] G. Aad et al. (ATLAS Collaboration), Phys. Lett. B **716**, 1 (2012);

S. Chatrchyan et al. (CMS Collaboration), Phys. Lett. B **716**, 30 (2012).

[2] G. Aad et al. (ATLAS and CMS Collaborations), JHEP **1608**, 045 (2016);

L. T. Hue, A. B. Arbuzov, N. T. K. Ngan, and H. N. Long, arXiv:1611.06801 [hep-ph];

M. Merchand and M. Sher, arXiv:1611.06887 [hep-ph];

M. Kumar, X. Ruan, R. Islam, A. S. Cornell, M. Klein, U. Klein and B. Mellado, arXiv:1509.04016 [hep-ph];

M. Kawasaki, K. Mukaida, and T. T. Yanagida, Phys. Rev. D **94**, no. 6, 063509 (2016);

C. Pallis, JCAP **1610**, no. 10, 037 (2016);

J. Baglio, Phys. Lett. B **764**, 54 (2017);

O. Evnin and R. Nivesvivat, arXiv:1604.00521 [nlin.SI];

A. L. Maroto and F. Prada, Phys. Rev. D **90**, no. 12, 123541 (2014), Erratum: [Phys. Rev. D **93**, no. 6, 069904 (2016)];

R. Gröber, arXiv:1611.07391 [hep-ph];

R. Romero and J. Besprosvany, arXiv:1611.07446 [hep-ph];

Z. Chen, Y. Yang, M. Ruan, D. Wang, G. Li, S. Jin, and Y. Ban, arXiv:1601.05352 [hep-ex];

A. Basirnia, S. Macaluso, and D. Shih, arXiv:1605.08442 [hep-ph];

R. Barbieri, L. J. Hall, and K. Harigaya, arXiv:1609.05589 [hep-ph];

A. Angelescu and G. Arcadi, arXiv:1611.06186 [hep-ph];

V. Prilepina and Y. Tsai, arXiv:1611.05879 [hep-ph];

G. C. Dorsch, S. J. Huber, T. Konstandin, and J. M. No, arXiv:1611.05874 [hep-ph];

A. Haarr, A. Kvellestad, and T. C. Petersen, arXiv:1611.05757 [hep-ph];

M. Spannowsky and C. Tamarit, arXiv:1611.05466 [hep-ph];

L. M. Carpenter, T. Han, K. Hendricks, Z. Qian, and N. Zhou, arXiv:1611.05463 [hep-ph];

C. Englert, K. Nordström, K. Sakurai, and M. Spannowsky, arXiv:1611.05445 [hep-ph].

[3] K.A. Olive et al. (Particle Data Group), Chin. Phys. C **38**, 090001 (2014) and 2015 update.

[4] G. Aad et al. (ATLAS and CMS Collaborations), arXiv:1606.02266 [hep-ex].

[5] G. Aad et al. (ATLAS Collaboration), arXiv:1506.05669v1 [hep-ex].

[6] V. Khachatryan et al. (CMS Collaboration), Phys. Rev. D **92**, no. 1, 012004 (2015).

[7] T. V. Zagoskin and A. Y. Korchin, JETP **149**, 770 (2016).

[8] A. Pilaftsis, C.E.M. Wagner, Nucl. Phys. B **553**, 3 (1999).

[9] V. Barger, P. Langacker, M. McCaskey et al., Phys. Rev. D **79**, 015018 (2009).

[10] G.C. Branco, P.M. Ferreira, L. Lavoura et al., Phys. Rep. **516**, 1 (2012).

[11] A. Bredenstein, A. Denner, S. Dittmaier and M. M. Weber, Phys. Rev. D **74**, 013004 (2006).

[12] S. Dittmaier et al. (LHC Higgs Cross Section Working Group Collaboration), doi:10.5170/CERN-2011-002, arXiv:1101.0593 [hep-ph].

[13] LHC Higgs Cross Section Working Group,
https://twiki.cern.ch/twiki/bin/view/LHCPhysics/CERNYellowReportPageBR3.

[14] M. Gasperini, Phys. Lett. B **327**, 214 (1994).

[15] S. Bolognesi, Y. Gao, A. V. Gritsan et al., Phys. Rev. D **86**, 095031 (2012).

[16] I. Anderson, S. Bolognesi, F. Caola et al., Phys. Rev. D **89**, no. 3, 035007 (2014).

[17] A. Soni and R. M. Xu, Phys. Rev. D **48**, 5259 (1993).

[18] V. A. Novikov, L. B. Okun, A. N. Rozanov, and M. I. Vysotsky, Rept. Prog. Phys. **62**, 1275 (1999).

[19] K.A. Olive et al. (Particle Data Group), Chin. Phys. C **38**, 090001 (2014).